# Progress in disruption prevention for ITER

**E.J. Strait**[1]**, J.L. Barr**[1]**, M. Baruzzo**[2]**, J.W. Berkery**[3]**, R.J. Buttery**[1]**,
P.C. de Vries**[4]**, N.W. Eidietis**[1]**, R.S. Granetz**[5]**, J.M. Hanson**[3]**,
C.T. Holcomb**[6]**, D.A. Humphreys**[1]**, J.H. Kim**[7]**, E. Kolemen**[8]**,
M. Kong**[9]**, M.J. Lanctot**[1,a]**, M. Lehnen**[4]**, E. Lerche**[10,11]**, N.C. Logan**[8]**,
M. Maraschek**[12]**, M. Okabayashi**[8]**, J.K. Park**[8]**, A. Pau**[13]**, G. Pautasso**[12]**,
F.M. Poli**[8]**, C. Rea**[5]**, S.A. Sabbagh**[3]**, O. Sauter**[9]**, E. Schuster**[14]**,
U.A. Sheikh**[9]**, C. Sozzi**[15]**, F. Turco**[3]**, A.D. Turnbull**[1]**, Z.R. Wang**[8]**,
W.P. Wehner**[14]** and L. Zeng**[16]

[1] General Atomics, PO Box 85608, San Diego, CA 92186-5608, United States of America
[2] Consorzio RFX, corso Stati Uniti 4, 35127 Padova, Italy
[3] Columbia University, New York, NY 10027, United States of America
[4] ITER Organization, Route de Vinon sur Verdon, 13067 St Paul Lez Durance, France
[5] Plasma Science and Fusion Center, Massachusetts Institute of Technology, Cambridge, MA, United States of America
[6] Lawrence Livermore National Laboratory, Livermore, CA 94551, United States of America
[7] National Fusion Research Institute, Daejon, Korea, Republic of
[8] Princeton Plasma Physics Laboratory, Princeton, NJ 08543, United States of America
[9] École Polytechnique Fédérale de Lausanne (EPFL), Swiss Plasma Center (SPC), CH-1015 Lausanne, Switzerland
[10] CCFE Fusion Association, Culham Science Centre, Abingdon, United Kingdom of Great Britain and Northern Ireland
[11] LPP-ERM/KMS, Association EUROFUSION-Belgian State, TEC partner, Brussels, Belgium
[12] Max-Planck-Institute für Plasma Physik, D-85748, Garching, Germany
[13] Electrical and Electronic Engineering Department, University of Cagliari, 09123 Cagliari, Italy
[14] Lehigh University, Bethlehem, PA 18015-3085, United States of America
[15] Instituto di Fisica del Plasma—Universita degli Studi di Milano-Bicocca, Milan, Italy
[16] Institute of Plasma Physics, Chinese Academy of Sciences, Hefei 230031, People's Republic of China

E-mail: strait@fusion.gat.com

CrossMark

## Abstract

Key plasma physics and real-time control elements needed for robustly stable operation of high fusion power discharges in ITER have been demonstrated in recent research worldwide. Recent analysis has identified the current density profile as the main drive for disruptive instabilities in discharges simulating ITER's baseline scenario with high and low external torque. Ongoing development of model-based profile control and active control of magnetohydrodynamic instabilities is improving the stability of multiple scenarios. Significant advances have been made toward real-time physics-based prediction of instabilities, including path-oriented analysis, active sensing, and machine learning techniques for prediction that are beginning to go beyond simple disruption mitigation trigger applications. Active intervention contributes to prevention of disruptions, including forced rotation of magnetic islands to prevent wall locking, and localized heating/current drive to shrink the islands. Stable discharge rampdowns have been achieved with the fastest ITER-like scaled current ramp rates, while maintaining an X-point configuration. These elements are being integrated into stable operating scenarios and new event-handling systems for off-normal events in order to develop the physics basis and techniques for robust control in ITER.

[a] Present address: U.S. Department of Energy, Washington, DC 20585-1290, United States of America

## 1. Introduction

The large thermal and magnetic energy contained in a full-performance discharge means that ITER must have an exceedingly low rate of disruptions by the time it reaches DT operation. A disruption budget [1] will be part of the ITER's operating plan [2], in order to track the cumulative effects of all disruptions. Although early operation at reduced parameters will allow more leeway for disruptions, unmitigated disruptions at currents above 8.4 MA may be severe enough (Category III) to be tolerable only once or twice in the machine's lifetime [3]. Thus, as experiments advance toward the planned current of 15 MA, the tolerance for unmitigated disruptions is expected to become of the order 1 in $10^4$ discharges. Figure 1 shows one possible scenario for the evolution of ITER's disruption rate [1]. After an initial learning curve at reduced parameters, by the time full fusion power operation is reached the allowable disruption rate per discharge is only 1%, and those few disruptions must be mitigated with 95%–99% accuracy. That is, nearly disruption-free operation will be required, *in addition to* highly reliable mitigation of any disruptions that do occur [4]. Uncertainties in prediction [5] and mitigation [6] of runaway electrons in ITER disruptions may place an even higher premium on disruption-free operation.

Sustaining a low disruptivity tokamak plasma is fundamentally a plasma control problem. Beginning with a minimally disruptive target scenario, continuously-operating algorithms in the plasma control system must be able to regulate the plasma state to maintain the desired operating point, with passive stability to as many potentially disruptive modes as possible. Any remaining potentially disruptive modes must be actively and robustly stabilized. In addition to quantifiably robust continuous algorithms, the control system must be able to detect and respond asynchronously to hardware faults and off-normal plasma conditions ('exceptions' in ITER terminology) [7, 8] in such a way as to prevent the exception from leading to a disruption. However, the plant and the nominal scenario should be so reliable that exceptions are extremely rare. Disruption mitigation must also be integrated into the plasma control system [9], but is outside the scope of this paper. In ITER, disruption mitigation should be a rarely-used last resort.

This paper provides an overview of recent research toward the goal of disruption-free operation. Section 2 discusses progress in identifying stable operating scenarios and robust control to maintain the desired operating state. Section 3 describes real-time algorithms that detect off-normal conditions, or predict that an instability will occur later in the discharge. Section 4 describes active intervention by various means to enable recovery of stable operation in the same scenario or an alternate one (maximizing the physics productivity of the discharge), or allow a controlled termination of the discharge.

These elements contribute to an integrated control solution, capable of robustly maintaining stable plasma conditions, or recognizing and responding to off-normal and fault events so as to reliably prevent disruptions (section 5).

## 2. Plasma configuration control

Reliable operation of ITER (and burning plasmas beyond ITER) requires a robustly stable, stationary operating state. Active control measures, up to and including a rapid shutdown by massive impurity injection, must be available to recover from off-normal conditions and prevent a disruption, or mitigate the severity of a disruption. However, it is clear that high reliability is needed in the normal operating state, so that the use of these safeguards is very rare. This is achieved through the selection of a stable plasma configuration, controls to achieve and maintain that configuration, stable paths to access the configuration at the beginning of the discharge and to exit from it at the end, and (where needed) active stabilization to extend the stability limits.

Optimization of the equilibrium configuration has been shown to improve the stability of zero torque ITER-like discharges. Previously, many such discharges in DIII-D disrupted due to tearing modes, and in general neoclassical tearing mode (NTM) stability appeared to become poorer as neutral beam torque was reduced [10]. In JET, NTMs were the largest single cause of disruption with the carbon wall [11], and could enhance core accumulation of impurities in operation with the ITER-like wall [12]. Recent DIII-D results have shown that tearing instabilities in ITER baseline scenario plasmas are related to the shape of the current density profile around the $q = 2$ surface. A deeper current 'well' between the ohmic current in the core and the bootstrap current at the edge is correlated with greater instability [13] (see figure 2).

In addition to the existence of a stable operating state, it is essential to have controls that will maintain the discharge in that state. Tokamak plasma control is complex, with nonlinear, coupled processes to be controlled, and possible bifurcations of the plasma state, putting a premium on integrated, model-based control [14]. The advent of transport simulations that can operate faster than real time [15] will be important for discharge monitoring and control. Simultaneous control of plasma pressure and safety factor using model-based control has been tested in a common environment [16] in TCV using several different controllers, [17–20]. In DIII-D, as shown in figure 3, a model-based feedforward + feedback algorithm [21] controls both neutral beams and gyrotrons to achieve simultaneous targets of plasma energy and a current density profile with high minimum safety factor $q_{min}$, in development of discharges for non-inductive operation [22]. Model-based control may be applicable to other scenarios as well.
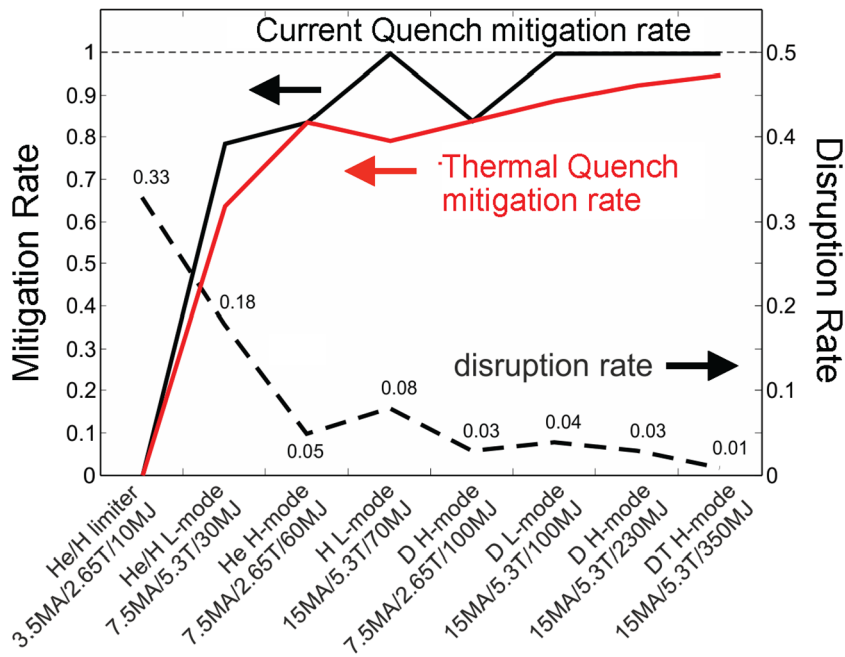
**Figure 1.** A potential scenario for ITER's allowable disruption rate and required mitigation rates, over the evolution of the planned research. Reproduced with permission from [1].
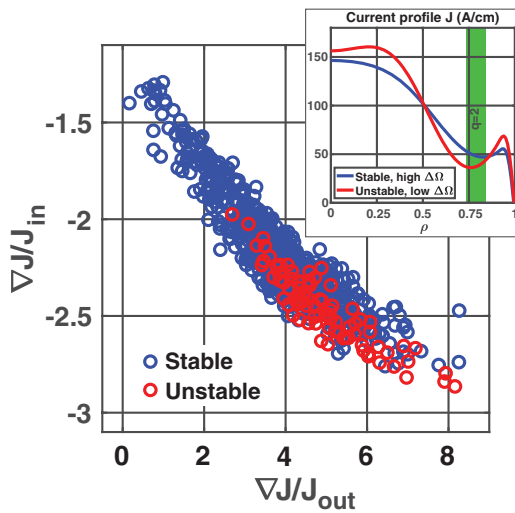


**Figure 2.** Current density gradient inside and outside the minimum or 'well' of current density near the $q = 2$ surface at $\rho \sim 0.76$–$0.81$ (see inset) in DIII-D discharges simulating the ITER baseline scenario. Colours indicate discharges stable (blue) or unstable (red) to $m/n = 2/1$ tearing modes. Reproduced courtesy of IAEA. Figure from [13]. Copyright 2018 IAEA.



**Figure 3.** Demonstration in DIII-D of a feedforward + feedback $q$-profile control scheme with model-based optimization, achieving a target profile with $q_{min} = 1.9$ while tracking a target value for plasma energy W.

Impurities can lead to instabilities and disruptions by altering the evolution of the pressure and current density profiles. In the initial operation of JET with an ITER-like metallic wall, disruptions were often caused by high impurity radiation from the plasma core, causing broadening of the current density profile that led to tearing modes [23, 24]. Disruptivity is reduced by using central electron heating with ion cyclotron resonance heating (ICRH) to improve the central power balance and reduce core impurity accumulation [23], perhaps similar to the use of central electron cyclotron resonance heating (ECRH) in ASDEX Upgrade with an all-tungsten wall [25]. The JET

disruption mitigation system is now in routine use, in many cases triggered by the onset of a locked tearing mode [26].

Maintaining a stable operating state may include extending the bounds of stable operation through direct control of instabilities. Real time active tracking and control of NTMs is well established, but recent analysis [27] indicates that the presence of ITER's blanket modules can cause $m/n = 2/1$ tearing modes to lock in a time significantly shorter than previous estimates that considered only the vacuum vessel wall. If active NTM stabilization is required, this result reduces the time available

**Figure 4.** Comparison of two H-mode discharges in JET with constant (left) and 3 Hz modulated (right) ICRF heating, illustrating the reliable sawtooth pacing and total suppression of the $n = 2$ MHD activity in the latter. (*a*) Auxiliary heating power; (*b*) electron temperature; (*c*) $n = 2$ MHD mode amplitude. Reproduced courtesy of IAEA. Figure from [36]. © 2017 Koninklijke Militaire School.



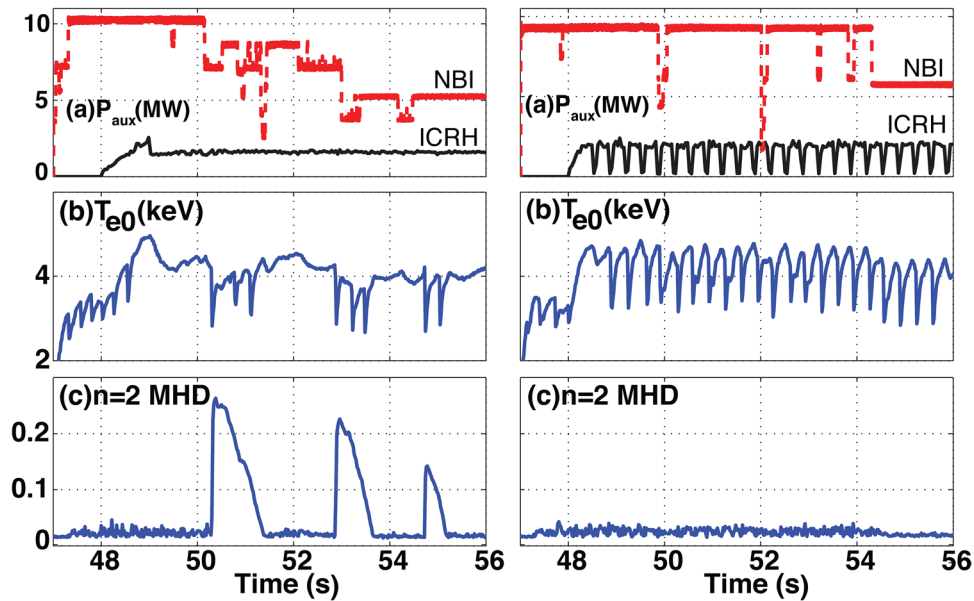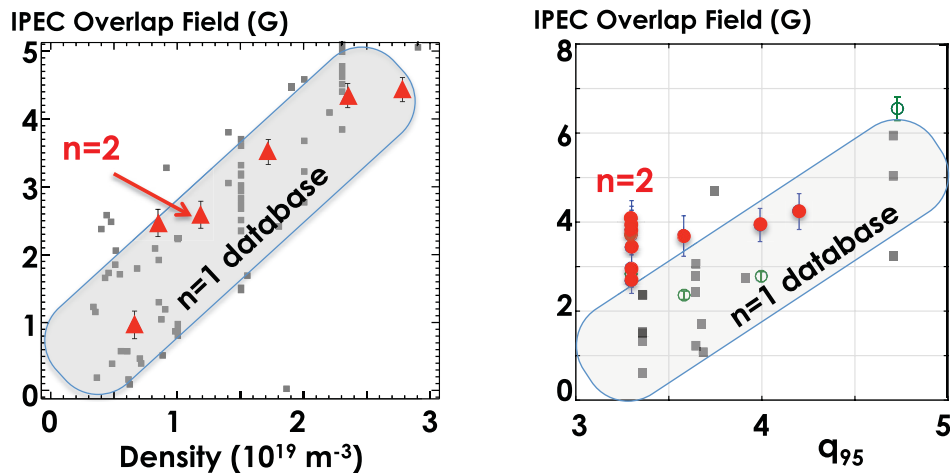**Figure 5.** Density dependence (left panel, DIII-D data) and $q_{95}$ dependence (right panel, EAST data) of the critical 'overlap' amplitude for $n = 2$ field penetration in Ohmic discharge, compared to $n = 1$ thresholds for similar discharges in DIII-D, KSTAR, JET, and (left panel only) NSTX and C-MOD. Reprinted from [37], with the permission of AIP Publishing.

for re-aiming gyrotrons to suppress the mode after detection, and increases the attractiveness of continuous electron cyclotron current drive (ECCD) applied at the rational surface to maintain NTM stability. The estimated power requirement of about 5 MW for pre-emptive stabilization of the 2/1 mode is consistent with ITER's electron cyclotron (EC) system, and would still allow demonstration of a fusion gain of $Q = 10$ [28]. Small-amplitude sweeping of the deposition location across the rational surface can reduce the requirements for accuracy of aiming, as first tested on TCV [29, 30] and later on ASDEX Upgrade [31]. Alternatively, a recently demonstrated fast resonant diplexer [32] could allow some gyrotrons to switch as needed between central heating/current drive and NTM control, without delay.

A need for control of the sawtooth instability is also anticipated in ITER, in order to avoid long period sawteeth with large amplitude crashes that could trigger an NTM instability [33], and several schemes using ECCD or ion cyclotron range of frequency (ICRF) heating have been proposed [34]. Controlled sawteeth and edge-localized modes (ELMs) can also improve disruptivity by flushing impurities out of the core and edge, respectively. Recent JET experiments have shown that the sawtooth period can be controlled with low field side ICRF heating (as will be available in ITER) near the $q = 1$ surface [35], and that sawtooth pacing can be achieved with modulated central ion cyclotron heating [36], a method that is less sensitive to the deposition location. Figure 4 shows an example where irregular sawteeth repeatedly seed an $n = 2$ tearing mode, but pacing at a higher rate using modulated central ICRH reduces the sawtooth period and eliminates the seeding. Further work is needed to validate ICRF sawtooth control in ITER-relevant high-confinement (H-mode) discharges.

Equilibrium control for stable operation includes non-axisymmetric aspects of the equilibrium. A large body of literature exists on the topic of $n = 1$ error fields, and ITER will include external non-axisymmetric coils for $n = 1$ error field compensation. However, as seen in figure 5, recent data from DIII-D and EAST show that the threshold for $n = 2$ error field penetration and driven reconnection may be comparable to that of $n = 1$ error fields [37]. This result suggests that the use of the in-vessel coils for $n = 2$ error field correction should be kept as an option for ITER, since the external correction will be hard-wired for $n = 1$. More complete data are needed to characterize the scaling of thresholds for $n = 2$ error field penetration in existing devices and to establish criteria for $n = 2$ error field control in ITER.

High beta, high $q_{min}$ discharges in ITER's steady state scenario are expected to exceed the no-wall ideal magnetohydrodynamic (MHD) kink stability limit. Despite the predicted stabilizing effects of particle-orbit resonances, active feedback control of non-axisymmetric fields for stabilization of the resistive wall mode or dynamic error field correction may be needed in this regime, in order to avoid instabilities leading to beta collapse and, in some cases, disruption. Experiments on NSTX [38] and DIII-D [39] have shown that feedback stabilization can indeed extend the stable operating range toward the ideal-wall limit (the theoretical maximum). Advanced state space control algorithms can achieve stabilization with external coil arrays [38, 40].

## 3. Real-time disruption warnings

Achieving a low rate of disruptions requires the ability to recognize or anticipate exceptions (i.e. conditions and events that are likely to lead to a disruption) in real time, and to take action that enables a return to normal operation or a controlled shutdown. It is important to distinguish such warnings from those that trigger a rapid shutdown by the disruption mitigation system; the latter require only a short warning time, perhaps as little as 30 ms before the thermal quench [4], and a binary output. In contrast, in order to allow the discharge to continue, notification of an exception must include information about the nature of the exception, enabling a control decision on a course of action using available actuators, and must occur early enough that the control system has time to change the evolution of the discharge. Potential solutions to this problem include 'physics-driven' methods based on a qualitative or quantitative model of the physical processes that would ultimately lead to an instability, and 'data-driven' or machine learning methods, where statistical analysis of a large database of discharges yields empirical correlations between measured data and instabilities. This is an area of rapid development in physics and mathematics.

To date, most real-time systems have used one or more single-parameter physics-based detectors (e.g. MHD mode amplitude, radiated power fraction, global energy confinement level, ...) to trigger a disruption mitigation system when a specified threshold is passed, or (with a lower threshold) to initiate more benign preventive actions. For example, routine JET disruption detection is based on detection of high levels
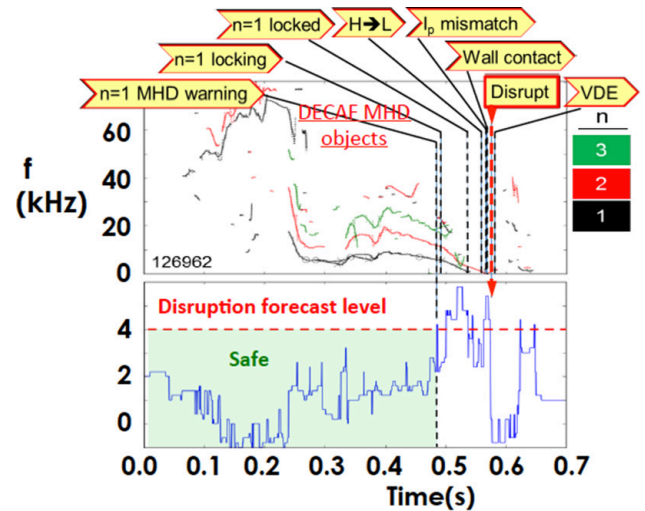


**Figure 6.** Upper panel: DECAF decomposition of rotating MHD in an NSTX discharge, with the timing of various events identified by DECAF on the path toward disruption. Lower panel: total MHD warning signal, based on the event chain identified at the top of the figure. Reproduced with permission from [46].

of MHD activity and radiation peaking, precursors to the thermal collapse, as well as large plasma current excursions or voltage spikes, following the thermal spike and signalling the start of the current quench [41]. Analysis of a multi-machine database [42] has provided a basis for normalizing the critical locked mode amplitude for disruption, independent of machine size, while analysis of a DIII-D database [43] shows that the proximity of the outer edge of the island to the plasma surface is a key factor in whether a locked mode leads to a disruption. Machine-learning approaches (discussed below) should be applicable to data analysis for optimization of these individual physics-based tests [44] and the control responses. Although each such test is specialized to certain classes of disruptions, multiple threshold tests can be combined with suitable weighting to make a more general warning system with a high success rate [45].

Path-oriented analysis seeks to identify specific chains of events that can lead to a disruption [11]. Detection of an event or condition early in the chain could enable a warning signal in time for modification of the discharge before it becomes unstable. The disruption event characterization and forecasting (DECAF) code [46], now being used to analyze data from several devices, identifies multiple events that may precede a disruption and aims to predict other instabilities using validated physics models such as a reduced model for resistive wall mode stability with kinetic effects [47] or tearing mode torque balance bifurcation to a locked state [48]. In the NSTX discharge shown in figure 6, DECAF identifies the onset of a tearing instability and several subsequent events, all of which contribute to a rising disruption warning signal. Multiple variable tests in DECAF have produced early warnings on transport timescales, potentially allowing time for actions to prevent a disruption. Another path-oriented approach is described in [49], including a discussion of the sensor and actuator requirements. Figure 7 shows an example of this second approach in ASDEX Upgrade of discharge recovery after a warning of crossing the H-mode density limit
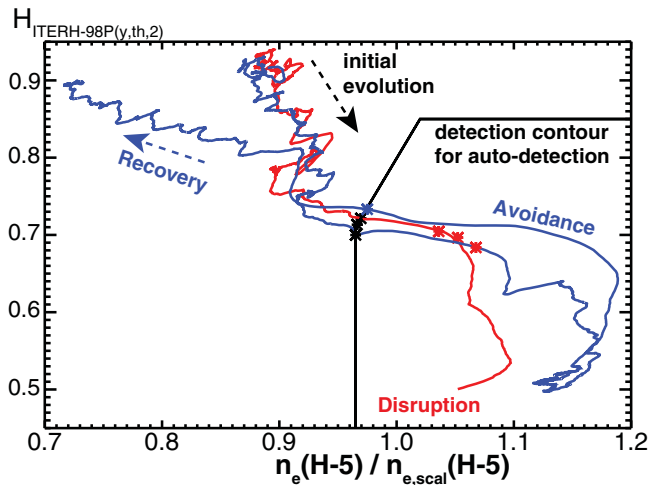
**Figure 7.** Operation diagram of H-mode density limit discharges in ASDEX-Upgrade, in terms of scaled energy confinement time versus scaled density. One discharges disrupts after crossing the density limit detection contour; the other is recovered by turning off gas fueling and applying ECCD. In all cases the proposed trigger threshold would have been early enough to safely avoid the approaching disruption. Reproduced from [49]. © 2017 Max-Planck-Institut for Plasmaphysics.

boundary. As a demonstration, TCV has isolated a specific path to disruption—impurity influx leading to an NTM that later locks—and developed controls to address each step of this path [50].

Data driven approaches such as the advance predictor of disruptions (APODIS) system [51] at JET have, so far, been tested mainly for binary warnings where the actuator is a disruption mitigation system. Adaptive methods to train an algorithm 'from scratch' have achieved satisfactory performance after only a few tens of disruptive shots [52–54]. Probabilistic predictors [54, 55] express output in terms of a likelihood of disruption rather than a binary classification, and the probabilistic approach has also been applied to forecasting the onset of a tearing mode [56]. Cross-device portability of data-driven algorithms (i.e. training the algorithm on one device and testing it on another) has had mixed success [57–59]. However, tests have shown that the accuracy can be significantly improved by adding to the training set as few as two discharges (one disrupting and one non-disrupting) from the target device [60]. Very recently deep-learning algorithms have begun to incorporate time-sequential data and higher-dimension data via advanced neural net methods with promising results, including more accurate cross-device predictions [61].

A key challenge for machine learning algorithms is to deliver detailed information about the exception that has been detected, so that the control system can generate an appropriate response to prevent the disruption. Work toward this goal is in progress. As seen in an example from EAST in figure 8, Random Forest algorithms can reveal the relative contributions of the various input data signals to the final disruption probability [59, 62]. Generative topographic mapping (GTM) reduces a complex multi-dimensional space of input data to a 2D or 3D space of safe and unstable regions, simplifying the tasks of classification, prediction, and control of instabilities
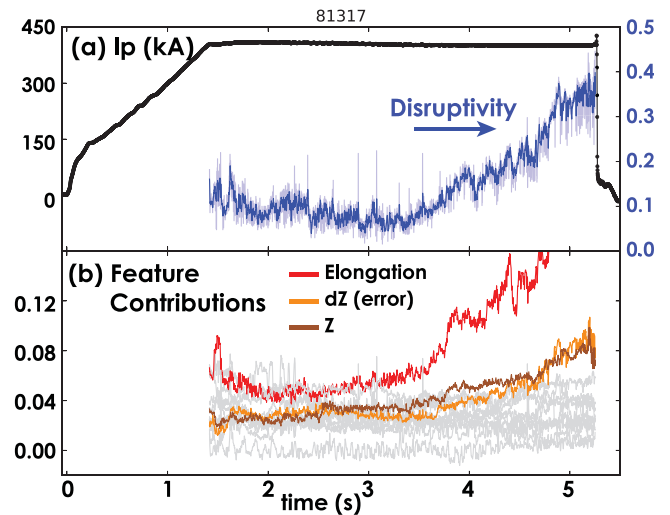


**Figure 8.** (*a*) Disruptivity signal (blue curve) from a Random Forest machine-learning algorithm rises as an EAST discharge approaches a vertical displacement event (VDE) instability. (*b*) Relative importance of the 13 input signals. Rising traces indicate high importance for discharge elongation, vertical position, and vertical control error. Reproduced with permission from [59].
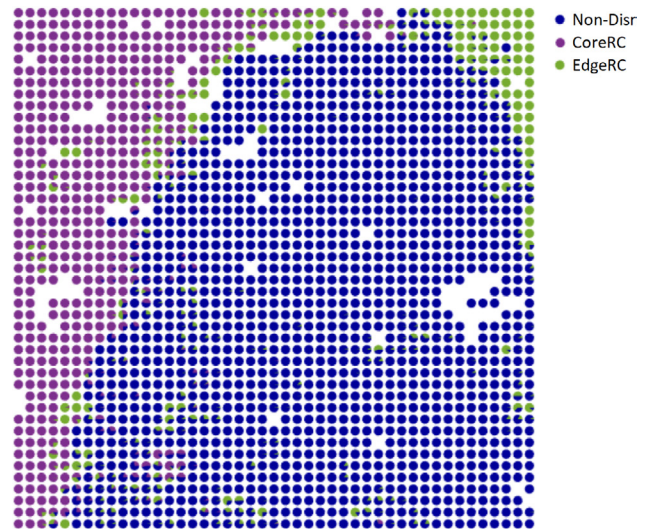


**Figure 9.** GTM of 5D JET data (peaking factors of electron temperature, electron density, and radiated power; internal inductance $\ell_i$; and $q_{95}/q_0$ ratio) to a 2D 'latent space'. Colours on the map distinguish stability regimes: core radiative collapse disruptions (CoreRC, magenta), edge radiative collapse (EdgeRC, green), and non-disrupting cases (blue). © 2018 IEEE. Reprinted, with permission, from [64].

[63, 64] (see figure 9). A proposed general approach [65] is to estimate the future trajectory of a discharge in the multidimensional space of input data—or perhaps in a reduced space such as that of figure 9—in order to project its future proximity to disruption boundaries and the time to collision with a boundary; any necessary actions would be based on the gradient of the decision function (e.g. disruption probability) and its dependence on the input data and available actuators. Translating these principles to a practical control scheme is a challenge for future work.

Methods for direct assessment of the plasma's stability are conceptually elegant, but are still in their infancy. Recent
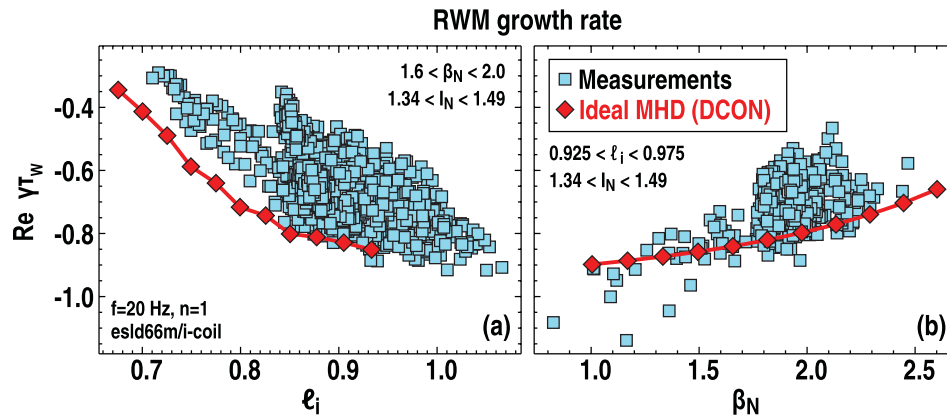
**Figure 10.** Stable ITER baseline scenario discharges in DIII-D: (*a*) $\ell_i$ and (*b*) $\beta_N$ dependences of the normalized RWM growth rate Re($\gamma\tau\omega$), comparing the values inferred from plasma response measurements (blue squares) with predictions of the linearized, ideal MHD, resistive wall dispersion relation (red diamonds). Reproduced with permission from [70].

advances in numerical methods and computing power have enabled first-principles calculation of ideal MHD stability in real time [66] and resistive stability in near real time [67]. Low-frequency active MHD spectroscopy offers the possibility of a direct real-time measurement of plasma stability. Originally developed for measuring the damping rates of ideal MHD modes [68], the technique has also shown a rising response correlated with the onset of tearing modes in ITER baseline scenario discharges in DIII-D [69]. As shown in figure 10, the dependence of the inferred damping rate on plasma parameters is in qualitative agreement with ideal MHD modeling [70], and this stability-related measurement has been used for closed-loop control of the heating power in an ITER baseline scenario discharge.

## 4. Response to off-normal conditions

A warning of an off-normal condition that is about to occur, or that is already in progress, is likely to require a response by the control system in order to prevent a disruption, with the response being determined by the nature of the off-normal condition. If feasible, continuing the discharge is preferable to ending it prematurely, and a controlled shutdown is preferable to a rapid termination. For example, the onset of a locked tearing mode is often a precursor to a disruption, but may allow time for other actions aimed at removing the instability and recovering normal operation, or limiting its growth during a controlled shutdown.

Forced rotation of magnetic islands by applied electromagnetic torque prevents locking to the wall, and reduces the island size. Several experiments [71–73], have demonstrated entrainment of a locked island by a rotating resonant magnetic perturbation (RMP) at frequencies in the 5–50 Hz range, limited in frequency by close coupling of the coils to the conducting vacuum vessel wall (figure 11). In the absence of strong wall currents, entrainment at several kHz has been achieved [74]. A modulated, non-rotating RMP is also proposed as a means of driving mode rotation [75]. During entrainment, the island maintains a saturated size, and in some
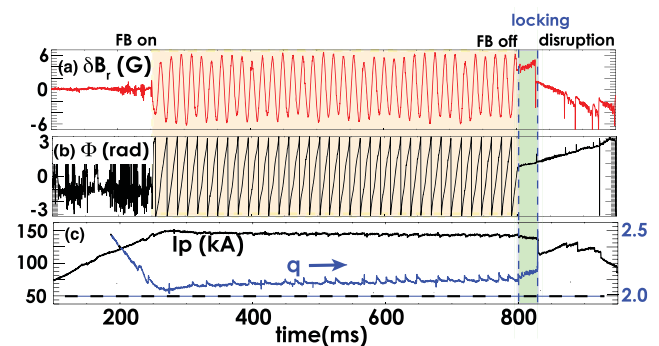


**Figure 11.** Long duration of post-unlocked sustainment of $m/n = 2/1$ mode in RFX-mod (#33748): (*a*) 2/1 $\delta B_r$ signal, (*b*) toroidal phase of the observed 2/1 mode component, (*c*) plasma current and safety factor $q_a$. Feedback-controlled magnetic perturbation drives the mode rotation during the orange-shaded interval. After feedback was turned off, the mode survived as a locked mode for a short interval (green) before disruption. Reproduced courtesy of IAEA. Figure from [72]. Copyright 2017 IAEA.

cases the H-mode edge pedestal is recovered [76]. Two-fluid modeling shows that island stabilization can occur with sufficient rotation of the RMP relative to the electron fluid [77, 78]. A reduced MHD simulation of the dynamics of island locking and entrainment [79] shows good qualitative agreement with experimental data [80]. A simple 0D model indicates that in ITER, the internal non-axisymmetric coils could entrain a locked island of 6–8 cm width at sub-10 Hz frequencies [73].

Pioneered in FTU, ASDEX Upgrade, and DIII-D, localized injection of EC power at the $q = 2$ surface has been developed as a means of preventing or postponing a disruption after a large amplitude locked mode is present—unlike the pre-emptive or small-amplitude NTM control by ECCD mentioned above in section 2. Joint experiments in FTU and ASDEX Upgrade show similar behavior in low-beta density limit disruptions and high-beta NTM-driven disruptions [81]. Rutherford equation analysis indicates that while the island is large, EC heating plays a larger role in stabilization than does current drive, and is less sensitive to the location of deposition. Real-time mirror steering has been included in the technique [82]. As shown in figure 12, TCV has demonstrated control of a large tearing mode destabilized by
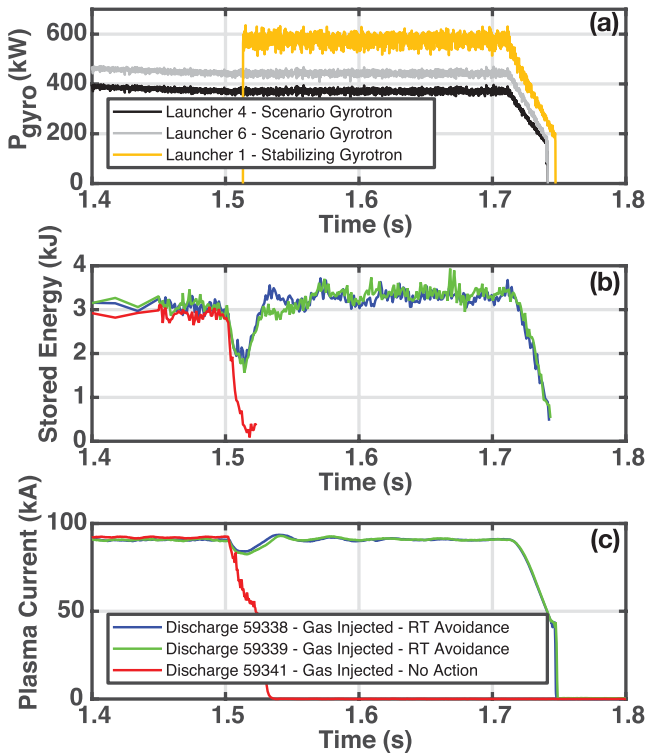
**Figure 12.** (*a*) Gyrotron power, (*b*) stored energy, and (*c*) plasma current for TCV discharges with real-time disruption avoidance control. Neon injection at $t = 1.5$ s induces a large tearing mode. ECCD targeted at $q = 2$ (panel (*a*), yellow curve), and triggered by SXR and locked mode signals, restores the plasma energy to pre-impurity levels through a combination of mode stabilization and island power balance (panels (*b*) and (*c*), blue and green curves). Red curves show a reference discharge with no action. Reproduced courtesy of IAEA. Figure from [50]. © EURATOM 2018.

impurity injection, before or after locking, using ECCD with real-time mirror steering based on real-time equilibrium reconstructions and ray tracing [50].

Forced island rotation has been combined with injection of EC power into the island for disruption prevention and discharge recovery [83]. A slow, controlled rotation of the island driven by the RMP, with modulated ECCD that is synchronized for deposition in the island O-point, avoids locking while maximizing the efficiency of stabilization by EC power. With this method, suppression of the island and recovery of H-mode operation has been demonstrated.

Stable discharge termination, whether planned or unplanned, is a critical element of disruption-free operation. An extensive study [84] of discharge terminations in existing tokamaks, in comparison with modeling for ITER, shows that ITER's expected trajectory may lie near the edge of the parameter space defined by present experiments. ITER's path is dictated by a rapid reduction of elongation while restricting the increase in internal inductance $\ell_i$, in order to maintain vertical stability. Recent experiments in EAST and DIII-D (figure 13) have demonstrated stable rampdowns with equivalent scaled $dI/dt$ up to the maximum expected for an unplanned 'soft landing' shutdown in ITER, including ITER-like X-point shape with reduced elongation, and low $\ell_i$ for vertical stability [85]. KSTAR has also demonstrated a safe rampdown scenario in response to off-normal events, using simplified shape and
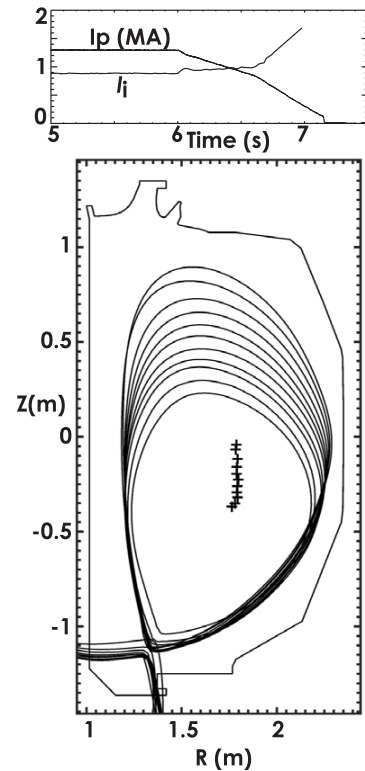


**Figure 13.** Stable ITER-like rampdown with X-point configuration, in DIII-D. Reproduced with permission from [85].

position controls for robustness [86], and TCV has tested an optimized rampdown trajectory developed from rapid plasma simulator (RAPTOR) simulations [87]. In these scenarios as well as in rampdowns of JET plasmas [88], an important feature is the use of modest auxiliary heating to maintain core power balance during the rampdown, while delaying the high to low confinement (H–L) transition until the plasma energy has been reduced. JET also utilizes ELM control (vertical kicks and pellet pacing) to minimize impurity accumulation [89]. A multi-machine database is being developed to improve physics-based simulations of the ITER rampdown [90].

## 5. Integrated control

The elements needed to minimize the occurrence of disruptions must be integrated, routine, and highly reliable in ITER. These include robustly stable operation, real-time identification of conditions likely to lead to a disruption, and the means to recover, switch to an alternative operating scenario, or terminate the discharge safely after an off-normal event. As discussed above, some building blocks are in hand in present experiments, while others are still under development. Conceptual design of exception handling for ITER and its integration into the plasma control system is in progress [7].

Many facilities are now starting to work toward more integrated control as will be needed in ITER. Key actuators are likely to be oversubscribed, and algorithms for actuator sharing based on generalized, device-independent logic are being developed [18]. Integrated control with actuator sharing has been demonstrated on ASDEX Upgrade [91, 92], and TCV [30, 93]. In the example from TCV shown in figure 14,
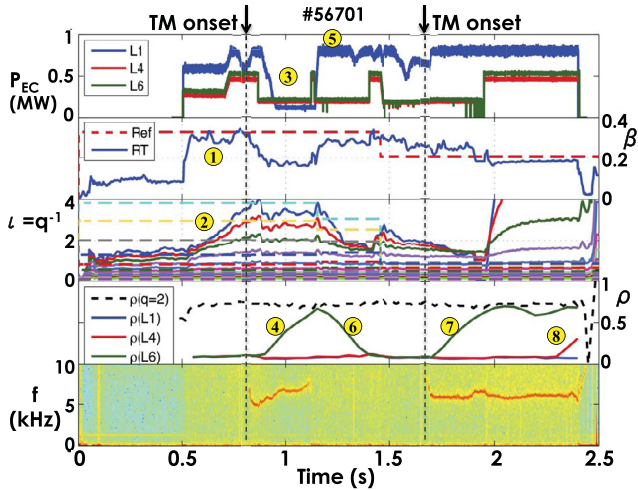
**Figure 14.** TCV discharge showing integrated control with actuator sharing. (1,2) During normal operation, central ECCD controls beta and $q$-profile. (3,4) After NTM onset, the heating power is reduced and one EC launcher is re-aimed to $q = 2$. (5,6) After stabilization of the NTM, heating power is raised and the launcher is returned to central current drive. (7,8) After onset of a second NTM, one EC launcher is re-aimed to $q = 2$. The EC pulse ends as a second launcher is being targeted to $q = 2$. Reproduced with permission from [93].

gyrotrons are used for simultaneous control of beta, and central q-profile, and switched to NTM control as needed.

With similar goals, DIII-D has implemented a generalized off-normal/fault response (ONFR) system to handle off-normal plasma events, and hardware faults [94]. Based on finite-state machine logic, the ONFR consists of multiple discrete operating states with rules for the transitions between states, and the rules may vary with the state. It provides the supervisory logic for recognition of off-normal conditions and appropriate actions to recover the discharge, change to an alternate mode of operation, or shut down the discharge. In a typical application, the ONFR system employs ECCD (continuous and pulsed) and forced island rotation by an applied $n = 1$ field to limit the growth of an $n = 1$ tearing mode, enabling a stable rampdown without disruption.

As the largest tokamak now in operation, JET faces many of the same issues as ITER. In preparation for the coming D–T campaign, JET has added controls to maintain the required operating point (including isotope ratio), carry out a controlled shutdown if the discharge is not evolving as planned, and trigger the disruption mitigation valve if a disruption is judged inevitable [95]. Work is in progress to ensure integration of these controllers with the rest of the control system [96]. The impact of central impurity accumulation on stable operation, including stable discharge termination, will be addressed by methods including improved detection of impurity accumulation, and optimization of ELM pacing by pellets and ICRH heating [97].

## 6. Discussion

The requirement of a disruption rate of $\leqslant 1\%$ in ITER is challenging. As a point of comparison, JET achieved an average

rate of 3.4% unintentional disruptions in the 2008–2010 time period [11], made possible mainly by development of reliable operating scenarios. However, the disruption rate increased significantly following the change from a carbon wall to an ITER-like metal wall [23]. Control of the edge tungsten transport and central power balance have improved disruptivity [96], and a disruption rate comparable to that of carbon-wall operation was realized in repeated operation of a specific discharge [26]. The low average disruption rates of carbon-wall operation have not been recovered for metal-wall operation in a broader parameter space, and this remains a challenge for ongoing research.

Many of the key elements of disruption-free tokamak operation have been demonstrated in present devices. The challenge now for present large and medium-size tokamaks is twofold. First, disruption prevention must move beyond proof-of-principle experiments to become an integrated part of the facility's normal operation, in order to demonstrate robustly stable operation. Routine, integrated disruption prevention over a range of plasma conditions (preferably with diagnostics and actuators similar to those available in ITER) will enhance the reliability and consistency of operation of today's devices, build confidence in the ability of tokamaks to operate without disruptions, and drive the control engineering development that is necessary for extension to ITER and other future devices. Second, methods of warning and prevention of disruptions must move beyond empirical criteria to establish well-supported physics bases, in order to enable application of the methods in future devices with little or no empirical training. This work is vital in preparation for disruption-free operation of ITER.

The actuators for control of the axisymmetric plasma in ITER (poloidal field coils, gas and pellet fueling systems, and heating and current drive systems) are similar to those in present facilities, as are the more specialized actuators for control of plasma stability (vertical stability coils, steerable launchers for localized EC current drive, and non-axisymmetric coils external and internal to the vacuum vessel). As in present facilities, the actuators will be controlled using input from diagnostics measuring spatially resolved profiles of temperature, density, and magnetic field in the plasma, as well as the external magnetic field, impurity radiation, etc. The close similarity in actuators and diagnostics should allow models and control methods developed in present experiments to guide the design of controls for operation of ITER without disruptions.

A key difference between ITER and present devices is that the response to many actuators is likely to be slower in ITER, owing to longer time scales for transport and magnetic relaxation. For example, the relaxation time for the current density profile scales as [98] $a^2/\eta$ (where $\eta$ is the plasma resistivity and $a$ the minor radius), and is expected to be of order $10^2$–$10^3$ s in ITER's $Q = 10$ discharges [2]. Consequently, the profiles—and the effect of control actions intended to change the profiles—could continue to evolve over the duration of the discharge. This result points to the importance of control scenarios that establish a stable current density profile during the discharge startup and robustly maintain it through the rest of the discharge. The long time scales for discharge evolution may be a benefit for predictive models that operate faster than

real time in order to look ahead as the discharge occurs, assess the impact of off-normal events, and foresee the results of possible corrective actions.

Theory and simulations will continue to be crucial in the development of disruption-free operation. Ideal MHD models have been successful in predicting stability limits and the response to external magnetic perturbations, and kinetic models have extended these capabilities to accurately predict the stability of resistive wall modes. In future work, nonlinear, nonideal models should be further extended, in order to predict the onset, growth, and saturation of metastable or linearly unstable tearing modes, for example, and to guide methods of maintaining or restoring stability through EC power [99, 100] or applied magnetic perturbations [77, 79]. Modeling is essential in order to develop the physics understanding that is needed to extend results in disruption warning and prevention from existing devices to ITER. In addition, a key goal of this research should be to validate 'reduced' models capable of predicting the discharge evolution and stability in real time.

## Acknowledgements

## Disclaimers

## ORCID iDs

J.L. Barr  https://orcid.org/0000-0001-7768-5931
N.W. Eidietis  https://orcid.org/0000-0003-0167-5053
M. Kong  https://orcid.org/0000-0002-2004-3513
M.J. Lanctot  https://orcid.org/0000-0002-7396-3372
N.C. Logan  https://orcid.org/0000-0002-3268-7359
M. Maraschek  https://orcid.org/0000-0002-3246-7559
A. Pau  https://orcid.org/0000-0002-7122-3346
F.M. Poli  https://orcid.org/0000-0003-3959-4371
C. Rea  https://orcid.org/0000-0002-9948-2649
O. Sauter  https://orcid.org/0000-0002-0099-6675
U.A. Sheikh  https://orcid.org/0000-0001-6207-2489
Z.R. Wang  https://orcid.org/0000-0002-7496-959X
L. Zeng  https://orcid.org/0000-0003-4968-1401

## References

[1] Lehnen M. *et al* 2016 Plasma disruption management in ITER *Preprint: 2016 IAEA Fusion Energy Conf. (Kyoto, Japan, 17–22 October 2016)* EX/P6-39

[2] ITER Organization 2018 ITER research plan within the staged approach (level III—provisional version) *ITER Technical Report* ITR-18-003 (www.iter.org/doc/www/content/com/Lists/ITER%20Technical%20Reports/Attachments/9/ITER-Research-Plan_final_ITR_FINAL-Cover_High-Res.pdf)

[3] Lehnen M. *et al* 2015 Disruptions in ITER and strategies for their control and mitigation *J. Nucl. Mater.* **463** 39

[4] de Vries P.C. *et al* 2016 Requirements for triggering the ITER disruption mitigation system *Fusion Sci. Technol.* **69** 471

[5] Boozer A.H. 2018 Pivotal issues on relativistic electrons in ITER *Nucl. Fusion* **58** 036006

[6] Konovalov S. *et al* 2016 Assessment of the runaway electron energy dissipation in ITER *Preprint: 2016 IAEA Fusion Energy Conf. (Kyoto, Japan, 17–22 October 2016)* TH/7-1

[7] Raupp G. *et al* 2017 Preliminary exception handling analysis for the ITER plasma control system *Fusion Eng. Des.* **123** 541

[8] Humphreys D. *et al* 2015 Novel aspects of plasma control in ITER *Phys. Plasmas* **22** 021806

[9] Pautasso G. *et al* 2018 The ITER disruption mitigation trigger: developing its preliminary design *Nucl. Fusion* **58** 036011

[10] Buttery R.J. *et al* 2008 The influence of rotation on the $\beta_N$ threshold for the 2/1 neoclassical tearing mode in DIII-D *Phys. Plasmas* **15** 056115

[11] de Vries P.C. *et al* 2011 Survey of disruption causes at JET *Nucl. Fusion* **51** 053018

[12] Hender T.C. *et al* 2016 The role of MHD in causing impurity peaking in JET hybrid plasmas *Nucl. Fusion* **56** 066002

[13] Turco F. *et al* 2018 The causes of the disruptive tearing instabilities of the ITER baseline scenario in DIII-D *Nucl. Fusion* **58** 106043

[14] Felici F. *et al* 2016 Real-time model-based plasma state estimation, monitoring and integrated control in TCV, ASDEX Upgrade and ITER *Preprint: 2016 IAEA Fusion Energy Conf. (Kyoto, Japan, 17–22 October 2016)* EX/P8-33

[15] Felici F. *et al* 2018 Real-time-capable prediction of temperature and density profiles in a tokamak using RAPTOR and a first-principle-based transport model *Nucl. Fusion* **58** 096006

[16] Maljaars E. *et al* 2017 Profile control simulations and experiments on TCV: a controller test environment and

results using a model-based predictive controller *Nucl. Fusion* **57** 126063

[17] Kim D. *et al* 2016 An active feedback plasma profile control approach applied to TCV plasmas and perspectives toward ITER *43rd EPS Conf. on Plasma Physics (Leuven, Belgium, 4–8 July 2016), Europhysics Conf. Abstracts* vol 40A p P4.069 (http://ocs.ciemat.es/EPS2016PAP/pdf/P4.069.pdf)

[18] Maljaars E. and Felici F. 2017 Actuator allocation for integrated control in tokamaks: architectural design and a mixed-integer programming algorithm *Fusion Eng. Des.* **122** 94

[19] Vu T. *et al* 2017 Plasma internal profile control using IDA-PBC: application to TCV *Fusion Eng. Des.* **123** 624

[20] Mavkov B. *et al* 2018 Experimental validation of a Lyapunov-based controller for the plasma safety factor and plasma pressure in the TCV tokamak *Nucl. Fusion* **58** 056011

[21] Wehner W. *et al* 2017 Optimal current profile control for enhanced repeatability of L-mode and H-mode discharges in DIII-D *Fusion Eng. Des.* **123** 513

[22] Wehner W.P. *et al* 2019 Physics-model-based real-time optimization for the development of steady-state scenarios at DIII-D *Nucl. Fusion* submitted

[23] de Vries P.C. *et al* 2014 The influence of an ITER-like wall on disruptions at JET *Phys. Plasmas* **21** 056101

[24] Angioni C. *et al* 2014 Tungsten transport in JET H-mode plasmas in hybrid scenario, experimental observations and modelling *Nucl. Fusion* **54** 083028

[25] Neu R. *et al* 2013 Overview on plasma operation with a full tungsten wall in ASDEX Upgrade *J. Nucl. Mater.* **438** S34

[26] Gerasimov S.N. *et al* 2018 Overview of disruptions with JET-ILW *Preprint: 2018 IAEA Fusion Energy Conf. (Gandhinagar, India, 22–27 October 2018)* EX/P1-24

[27] La Haye R.J. *et al* 2017 Effect of thick blanket modules on neoclassical tearing mode locking in ITER *Nucl. Fusion* **57** 014004

[28] Poli F.M. *et al* 2018 Electron cyclotron power management for control of neoclassical tearing modes in the ITER baseline scenario *Nucl. Fusion* **58** 016007

[29] Kim D. 2015 Real-time control of Sawteeth and NTMs in TCV and ITER *PhD Thesis* École Polytechnique Fédérale de Lausanne (https://infoscience.epfl.ch/record/205040/files/EPFL_TH6539.pdf)

[30] Kong M. *et al* 2019 Control of NTMs and integrated multi-actuator plasma control on TCV *Nucl. Fusion* accepted (https://doi.org/10.1088/1741-4326/ab1e1e)

[31] Maraschek M. *et al* 2015 Real-time control of MHD instabilities using ECCD in ASDEX Upgrade *Proc. 42nd EPS Conf. on Plasma Physics (Lisbon, Portugal, 22–26 June 2015), Europhysics Conf. Abstracts* vol 39E p P1.112 (http://ocs.ciemat.es/EPS2015PAP/pdf/P1.112.pdf)

[32] Kasparek W. *et al* 2016 NTM stabilization by alternating O-point EC current drive using a high-power diplexer *Nucl. Fusion* **56** 126001

[33] Chapman I.T. *et al* 2010 Empirical scaling of sawtooth period for onset of neoclassical tearing modes *Nucl. Fusion* **50** 102001

[34] Chapman I.T. *et al* 2013 Power requirements for electron cyclotron current drive and ion cyclotron resonance heating for sawtooth control in ITER *Nucl. Fusion* **53** 066001

[35] Graves J.P. *et al* 2015 Sawtooth control in JET with ITER relevant low field side resonance ion cyclotron resonance heating and ITER-like wall *Plasma Phys. Control. Fusion* **57** 014033

[36] Lerche E. *et al* 2017 Sawtooth pacing with on-axis ICRH modulation in JET-ILW *Nucl. Fusion* **57** 036027

[37] Lanctot M.J. *et al* 2017 Impact of toroidal and poloidal mode spectra on the control of non-axisymmetric fields in tokamaks *Phys. Plasmas* **24** 056117

[38] Sabbagh S.A. *et al* 2013 Overview of physics results from the conclusive operation of the national spherical torus experiment *Nucl. Fusion* **53** 104007

[39] Hanson J.M. *et al* 2017 Stability of DIII-D high-performance, negative central shear discharges *Nucl. Fusion* **57** 056009

[40] Clement M. *et al* 2018 H2 optimal control techniques for resistive wall mode feedback in tokamaks *Nucl. Fusion* **58** 046017

[41] Rimini F.G. *et al* 2015 The development of safe high current operation in JET-ILW *Fusion Eng. Des.* **96–7** 165

[42] de Vries P.C. *et al* 2016 Scaling of the MHD perturbation amplitude required to trigger a disruption and predictions for ITER *Nucl. Fusion* **56** 026007

[43] Sweeney R. *et al* 2017 Statistical analysis of $m/n = 2/1$ locked and quasi-stationary modes with rotating precursors at DIII-D *Nucl. Fusion* **57** 016019

[44] Sozzi C. *et al* 2018 Early identification of disruption paths for prevention and avoidance *Preprint: 2018 IAEA Fusion Energy Conf. (Gandhinagar, India, 22–27 October 2018)* EX/P1-22

[45] Gerhardt S.P. *et al* 2013 Detection of disruptions in the high-$\beta$ spherical torus NSTX *Nucl. Fusion* **53** 063021

[46] Sabbagh S.A. *et al* 2018 Disruption event characterization and forecasting in tokamaks *Preprint: 2018 IAEA Fusion Energy Conf. (Gandhinagar, India, 22–27 October 2018)* EX/P6-26

[47] Berkery J.W. *et al* 2017 A reduced resistive wall mode kinetic stability model for disruption forecasting *Phys. Plasmas* **24** 056103

[48] Berkery J.W. *et al* 2017 Characterization and forecasting of global and tearing mode stability for tokamak disruption avoidance *Proc. 44th EPS Conf. on Plasma Physics (Belfast, UK, 26–30 June 2017), Europhysics Conf. Abstracts* vol 41F p P1.138 (http://ocs.ciemat.es/EPS2017PAP/pdf/P1.138.pdf)

[49] Maraschek M. *et al* 2018 Path-oriented early reaction to approaching disruptions in ASDEX Upgrade and TCV in view of the future needs for ITER and DEMO *Plasma Phys. Control. Fusion* **60** 014047

[50] Sheikh U.A. *et al* 2018 Disruption avoidance through the prevention of NTM destabilization in TCV *Nucl. Fusion* **58** 106026

[51] Ratta G.A. *et al* 2010 An advanced disruption predictor for JET tested in a simulated real-time environment *Nucl. Fusion* **50** 025005

[52] Dormido-Canto S. *et al* 2013 Development of an efficient real-time disruption predictor from scratch on JET and implications for ITER *Nucl. Fusion* **53** 113001

[53] Vega J. *et al* 2014 Adaptive high learning rate probabilistic disruption predictors from scratch for the next generation of tokamaks *Nucl. Fusion* **54** 123001

[54] Murari A. *et al* 2018 Adaptive predictors based on probabilistic SVM for real time disruption mitigation on JET *Nucl. Fusion* **58** 056002

[55] Kleijwegt K. *et al* 2019 Disruption prediction using machine learning algorithms for DIII-D, *Nucl. Fusion* submitted

[56] Olofsson K.E.J. *et al* 2018 Event hazard function learning and survival analysis for tearing mode onset characterization *Plasma Phys. Control. Fusion* **60** 084002

[57] Windsor C.G. *et al* 2005 A cross-tokamak neural network disruption predictor for the JET and ASDEX Upgrade tokamaks *Nucl. Fusion* **45** 337

[58] Rea C. *et al* 2018 Disruption prediction investigations using machine learning tools on DIII-D and alcator C-mod *Plasma Phys. Control. Fusion* **60** 084004

[59] Granetz R.S. *et al* 2019 Machine learning for disruption warning on Alcator C-MOD, DIII-D, and EAST tokamaks *Nucl. Fusion* submitted

[60] Rattá G.A., Vega J. and Murari A. 2018 Viability assessment of a cross-tokamak AUG-JET disruption predictor *Fusion Sci. Technol.* **74** 13

[61] Kates-Harbeck J. *et al* 2019 Predicting disruptive instabilities in controlled fusion plasmas through deep learning *Nature* **568** 526

[62] Rea C. *et al* 2018 Initial results of a machine learning-based real time disruption predictor on DIII-D *Proc. 45th EPS*

*Conf. on Plasma Physics (Prague, Czech Republic, 2–6 July 2018), Europhysics Conf. Abstracts* vol 42A p P1.1076 (http://ocs.ciemat.es/EPS2018PAP/pdf/P1.1076.pdf)

[63] Cannas B. *et al* 2015 Automatic disruption classification in JET with the ITER-like wall *Plasma Phys. Control. Fusion* **57** 125003

[64] Pau A. *et al* 2018 A first analysis of JET plasma profile-based indicators for disruption prediction and avoidance *IEEE Trans. Plasma Sci.* **46** 2691

[65] Parsons M. 2017 Interpretation of machine-learning-based disruption models for plasma control *Plasma Phys. Control. Fusion* **59** 085001

[66] Glasser A.S., Kolemen E. and Glasser A.H. 2018 A Riccati solution for the ideal MHD plasma response with applications to real-time stability control *Phys. Plasmas* **25** 032507

[67] Glasser A.S. and Kolemen E. 2018 A robust solution for the resistive MHD toroidal $\Delta'$ matrix in near real-time *Phys. Plasmas* **25** 082502

[68] Reimerdes H. *et al* 2004 Measurement of the resistive-wall-mode stability in a rotating plasma using active MHD spectroscopy *Phys. Rev. Lett.* **93** 135002

[69] Turco F. *et al* 2016 Current density and rotation profiles govern the stability of the ITER baseline scenario in DIII-D; predictive transport simulations capture the confinement degradation due to direct electron heating *Preprint: 2016 IAEA Fusion Energy Conf. (Kyoto, Japan, 17–22 October 2016)* EX/P3-14

[70] Hanson J.M. *et al* 2018 Understanding and controlling the ITER baseline plasma response *Proc. 45th EPS Conf. on Plasma Physics (Prague, Czech Republic, 2–6 July 2018), Europhysics Conf. Abstracts* vol 42A p P2.1110 (http://ocs.ciemat.es/EPS2018PAP/pdf/P2.1110.pdf)

[71] Paccagnella R. *et al* 2016 Entrainment of MHD modes in ASDEX Upgrade using rotating non-axisymmetric perturbation fields *Proc. 43rd EPS Conf. on Plasma Physics (Leuven, Belgium, 4–8 July 2016), Europhysics Conf. Abstracts* vol 40A p P1.027 (http://ocs.ciemat.es/EPS2016PAP/pdf/P1.027.pdf)

[72] Okabayashi M. *et al* 2017 Avoidance of tearing mode locking with electromagnetic torque introduced by feedback-based mode rotation control in DIII-D and RFX-mod *Nucl. Fusion* **57** 016035

[73] Choi W. *et al* 2018 Feedforward and feedback control of locked mode phase and rotation in DIII-D with application to modulated ECCD experiments *Nucl. Fusion* **58** 036022

[74] Jin H. *et al* 2015 Locked mode unlocking by rotating resonant magnetic perturbations in J-TEXT tokamak *Plasma Phys. Control. Fusion* **57** 104007

[75] Hu Q. and Yu Q. 2016 Suppressing magnetic island and accelerating its rotation by modulated resonant magnetic perturbation *Nucl. Fusion* **56** 034001

[76] Okabayashi M. *et al* 2016 Physics of unlocked tearing modes and disruption avoidance by feedback-based electromagnetic torque injection *Preprint: 2016 IAEA Fusion Energy Conf. (Kyoto, Japan, 17–22 October 2016)* p EX/P3-16

[77] Yu Q. *et al* 2018 Suppressing magnetic island growth by resonant magnetic perturbation *Nucl. Fusion* **58** 054003

[78] Yu Q. *et al* 2018 NTM excitation by sawtooth crashes and the suppression of their onset by resonant magnetic perturbation *Preprint: 2018 IAEA Fusion Energy Conf. (Gandhinagar, India, 22–27 October 2018)* TH/P5-19

[79] Inoue S. *et al* 2018 Dependence of mode locking/unlocking on frequency of rotating 3D field and its experimental application for active locked mode avoidance *Preprint: 2018 IAEA Fusion Energy Conf. (Gandhinagar, India, 22–27 October 2018)* TH/P5-24

[80] Okabayashi M. *et al* 2018 Critical processes of tearing mode entrainment in the presence of a static error field *Preprint: 2018 IAEA Fusion Energy Conf. (Gandhinagar, India, 22–27 October 2018)* EX/P6-25

[81] Esposito B. *et al* 2011 Disruption avoidance by means of electron cyclotron waves *Plasma Phys. Control. Fusion* **53** 124035

[82] Granucci G. *et al* 2015 Stable operation at disruptive limits by means of EC at ASDEX Upgrade *Proc. 42nd EPS Conf. on Plasma Physics (Lisbon, Portugal, 22–26 June 2015), Europhysics Conf. Abstracts* vol 39E p P1.108 (http://ocs.ciemat.es/EPS2015PAP/pdf/P1.108.pdf)

[83] Volpe F.A. *et al* 2015 Avoiding tokamak disruptions by applying static magnetic fields that align locked modes with stabilizing wave-driven currents *Phys. Rev. Lett.* **115** 175002

[84] de Vries P.C. *et al* 2018 Multi-machine analysis of termination scenarios with comparison to simulations of controlled shutdown of ITER discharges *Nucl. Fusion* **58** 026019

[85] Barr J.L. *et al* 2018 Fast ITER-relevant low-disruptivity rampdowns in DIII-D and EAST *Preprint: 2018 IAEA Fusion Energy Conf. (Gandhinagar, India, 22–27 October 2018)* EX/P6-21

[86] Woo M.H. *et al* 2018 Implementation of the forced landing scheme under off-normal events in KSTAR *Fusion Eng. Des.* **128** 168

[87] Teplukhina A.A. *et al* 2017 Simulation of profile evolution from ramp-up to ramp-down and optimization of tokamak plasma termination with the RAPTOR code *Plasma Phys. Control. Fusion* **59** 124004

[88] Hobirk J. *et al* 2018 Analysis of plasma termination in the JET hybrid scenario *Nucl. Fusion* **58** 076027

[89] de La Luna E. *et al* 2018 Impact of ELM control in JET experiments on H-mode terminations with/without current ramp-down and implications for ITER *Preprint: 2018 IAEA Fusion Energy Conf. (Gandhinagar, India, 22–27 October 2018)* EX/2-1

[90] Poli F.M. *et al* 2018 The plasma current ramp-down in ITER: physics constraints on control *Preprint: 2018 IAEA Fusion Energy Conf. (Gandhinagar, India, 22–27 October 2018)* EX/P7-27

[91] Rapson C.J. *et al* 2017 Experiments on actuator management and integrated control at ASDEX Upgrade *Fusion Eng. Des.* **123** 603

[92] Kudlacek O. *et al* 2018 Actuator management development on ASDEX-Upgrade *Fusion Eng. Des.* accepted (https://doi.org/10.1016/j.fusengdes.2019.02.026)

[93] Kong M. *et al* 2017 Real-time control of neoclassical tearing modes and its integration with multiple controllers in the TCV tokamak *Paper Proc. 44th EPS Conf. on Plasma Physics (Belfast, UK, 26–30 June 2017), Europhysics Conf. Abstracts* vol 41F p P4.152 (http://ocs.ciemat.es/EPS2017PAP/pdf/P4.152.pdf)

[94] Eidietis N.W. *et al* 2018 Implementing a finite-state off-normal and fault response system for disruption avoidance in tokamaks *Nucl. Fusion* **58** 056023

[95] Lennholm M. *et al* 2017 Real time control developments at JET in preparation for deuterium-tritium operation *Fusion Eng. Des.* **123** 535

[96] Joffrin E. *et al* 2019 Overview of the JET preparation for deuterium–tritium operation *Nucl. Fusion* accepted (https://doi.org/10.1088/1741-4326/ab2276)

[97] Garzotti L. *et al* 2019 Scenario development for DT operation at JET *Nucl. Fusion* accepted (https://doi.org/10.1088/1741-4326/ab1cca)

[98] Mikkelsen D.R. 1989 Current relaxation time scales in toroidal plasmas *Phys. Fluids* B **1** 333

[99] Pratt J. *et al* 2016 Early evolution of electron cyclotron driven current during suppression of tearing modes in a circular tokamak *Phys. Plasmas* **23** 102507

[100] Lazzaro E. *et al* 2018 Physics conditions for robust control of tearing modes in a rotating tokamak plasma *Plasma Phys. Control. Fusion* **60** 014044